

Arsenite promotes intestinal tumor cell proliferation and invasion by stimulating epithelial-to-mesenchymal transition

Jia-liang Sun^{1,†}, Dan-lei Chen^{1,†}, Zhong-qian Hu^{1,2}, You-zhi Xu¹, Hao-shu Fang¹, Xin-yi Wang^{1,3}, Lixin Kan¹, and Si-ying Wang^{1,*}

¹Department of Pathophysiology; School of Basic Medical Sciences; Anhui Medical University; Hefei, Anhui, PR China; ²Department of Ultrasound; Zhongda Hospital; Southeast University; Nanjing, Jiangsu, PR China; ³Department of Clinical Medicine; Anhui Medical University; Hefei, Anhui, PR China

[†]These authors contributed equally to this work.

Keywords: colon cancer, arsenite (AS, As₂O₃), tumor invasion and proliferation, epithelial to mesenchymal transition (EMT)

Abbreviations: EMT, epithelial-mesenchymal transition; MTT, 3-[4,5-dimethyl-2-thiazolyl]-2,5-diPhenyl-2H-tetrazolium bromide; PI, propidium iodide; MMPs, matrix metalloproteinases; OD, optical density; PVDF, polyvinylidene difluoride membranes; DAPI, 4'-6-diamidino-2-phenylindole

Arsenite (AS) is a ubiquitous environmental element that is widely present in food, soil, and water. Environmental exposure to AS represents a major global health concern, because AS is a well-established human carcinogen. We hypothesize that low concentration of AS could enhance metastasis and proliferation of transformed cancer cells by promoting EMT. To test this hypothesis, we treated human colorectal cancer cells with low concentration of AS, and then measured the multiple readouts of cell viability, proliferation, migration, and adhesion *in vitro* and *in vivo*. Collectively, our data indeed strongly support our hypothesis and shed novel light into this important pathophysiological process. These novel insights are not only of high interests to basic cancer research, but may also have direct implications in cancer prevention and treatment.

Introduction

Human beings are exposed to arsenite (AS) through environmental, medical, and occupational sources. AS is well-established as a human carcinogen and it remains a major public health concern.¹ Acute and chronic AS exposure via drinking water has been reported in many countries of the world. There is sufficient epidemiological evidence to support a causal association between AS exposure and human disease. Long-term exposure to AS through contaminated drinking water increases the risk of skin, lung, bladder, liver, and prostate cancers.²⁻⁶ Although evidence for the carcinogenicity of AS in humans is strong, the underlying mechanisms of AS induced tumorigenesis are still unclear.

EMT normally refers to a specific physiological or pathophysiological phenomenon, which is characterized by the loss of polarity of epithelial cells and decreased adhesion with surrounding cells.^{7,8} Previous studies indicated that AS could induce cell malignant transformation through epithelial to mesenchymal transition (EMT);⁹ conversely, activation of the EMT has been implicated in the metastasis of human tumors, including skin.¹⁰

In our current study, we hypothesize that low concentration of AS could enhance metastasis and proliferation of transformed cancer cells by promoting EMT. To directly test this hypothesis,

we treated human colorectal cancer cells (HT-29) with low concentration of AS chronically or acutely, and then measured the *in vitro* and *in vivo* readouts of cell viability, proliferation, migration, and adhesion to determine whether the metastasis and proliferation of transformed cancer cells were enhanced. Further immunostaining with pan-epithelial and pan-mesenchymal markers was employed to determine whether enhanced EMT was indeed an underlying mechanism.

Overall, our data indeed strongly support the idea that AS promotes intestinal tumor cell proliferation and invasion by stimulating EMT. These novel insights could have direct implications for cancer prevention and treatment.

Results

Chronic exposure to AS promotes the proliferation of HT-29 cell lines

It has been established in the literature that a low concentration (1.0 μM) of AS induces anchorage-independent growth of HaCaT cells in soft agar.¹¹ In our current study, the HT-29 cell lines were exposed to 0 or 15 nM AS for 15 wk (AS30 passages) and 30 wk (AS60 passages). The viability of AS-treated cells was

*Correspondence to: Si-ying Wang; Email: sywang@ahmu.edu.cn

Submitted: 02/28/2014; Revised: 06/22/2014; Accepted: 06/22/2014; Published Online: 07/10/2014
<http://dx.doi.org/10.4161/cbt.29685>

determined by the MTT assay (Fig. 1A and B). We found that the numbers of viable cell in AS (60) group were always higher than that of AS (30) group, which in turn, were higher than control group.

Similarly, cell cycle study found that AS (60) cells re-entered cell cycle (S phase) at accelerated rate, comparing to AS (30) cells and control cells (Fig. 1C–E).

The increased colony number and colony size of in colony formation study provided additionally evidence to support that AS treated cells (AS [60] and AS [30] cells) have higher rates of proliferation (Fig. 1F–M), comparing to control cells.

Chronic exposure to AS enhances the migration and invasion of HT-29 cell lines

To further determine the effect of chronic exposure to AS on migration and invasion, 2D wound closure, and Transwell assay were performed (Fig. 2A–Q). In the wound healing assay, AS (60) cells closed the wound much faster than AS (30) cells, which in turn, is faster than control cells. In fact, 48 h after the scratch, the wound in AS (60) cells were completely closed (Fig. 2A–J), which was not found in any other group.

The invasive activity was further verified by a Transwell assay. As expected, similar trend was observed, i.e., the number of invading cells that migrated through the Matrigel was the greatest in AS (60) group. In contrast, fewer AS (30) cells have the same migration ability, and even fewer cells in control group migrated through the Matrigel. The intensity of violet staining was measured by the absorbance at 560 nm to quantify the invasive activity (Fig. 2K–Q).

Chronic exposure to AS promotes tumor growth in NOD/SCID mice

We next tested the capacity of tumorigenesis of AS treated cells in vivo. To this end, AS-treated cells were injected subcutaneously into the 6- to 8-wk-old NOD/SCID female mice (Fig. 3A). The AS (60) tumor began to be observed on day 10, and the growth of tumor accelerates from this time point onward. Up to day 40, the average volume of the AS (60) tumors was markedly larger than that in AS (30) group, which in turn was larger than the control tumors (Fig. 3B and C). Similar trend was observed in the final tumor weight (Fig. 3D). Together, our data suggested that chronic exposure to AS promoted the growth and metastasis of colon cancer cells in vivo.

EMT is involved in AS treated HT-29 cells

Literatures indicated that inhibition of cellular adhesive ability is associated with EMT.¹² Consistently, in the process of chronic AS exposure, we noted with great interest that AS treated HT-29 cells underwent a marked morphologic change, i.e., from epithelial to spindle-like mesenchymal morphology (Fig. 4A–C).

Our further study found that there was greater attenuation of cellular adhesive capacity, with prolonged exposure to AS (Fig. 4D). All these changes suggested that chronic exposure to AS may cause EMT.

To further confirm that the observed phenomenon indeed reflects bona fide EMT, we compared the expression of pan-epithelial (E-cadherin) and pan-mesenchymal (vimentin) markers in AS-treated cells through immunofluorescence staining. Our data indeed confirmed the EMT-associated shift of

the expression of the markers, i.e., after exposed to AS for 15 and 30 wk, the expression levels of E-cadherin was significantly decreased and the expression of vimentin were markedly increased. Furthermore, the transformed cells formed mesenchymal-like intercellular junctions (Fig. 4E–V). Overall, the morphological and molecular changes all suggested that HT-29 cells underwent an EMT process after prolonged AS exposure.

Acute exposure to AS also induces the EMT-like phenotypical shift

To test whether acute exposure to AS can also induce EMT-like phenotypical shift. Naïve HT-29 cells were exposed to AS in the short term, i.e., 0, 6, 12, and 24 h. We then examined the expression of E-cadherin and vimentin in treated cells by western blotting. We found that the E-cadherin level was decreased, while vimentin level was increased, similar to what we have observed in cells with prolonged AS exposure. To further explore whether other EMT related protein were also involved in the process, we next observed the expression of the matrix metalloproteinases MMP-3, MMP-9, the EMT related transcription factors ZEB-1, and nuclear β -catenin. It was of interest to note that all these EMT related protein were upregulated by AS (15 nM) treatment at the time of 12 h (Fig. 5A and B).

Discussion

Colorectal cancer has been a serious threat. For example, in China, the mortality of patients with colorectal tumor has been ranked fourth in the worldwide, followed by about 1 million newly diagnosed cases and nearly 608 000 deaths.^{13,14} Several studies have shown that the occurrence of colon cancer is the result of the interaction between genetic factors and environmental factors,^{15–18} i.e., environmental pollutants play key role in the process.^{19,20}

AS enters the body mainly through a variety of polluted foods and drinking water, and it can also be absorbed to the body through the skin or respiratory system. At least 90% of ingested AS are absorbed from gastrointestinal tracts, including colon. Non-conjugated trivalent arsenicals are highly reactive with thiol compounds and are easily converted to less toxic corresponding pentavalent arsenicals, mainly in the liver. But the specific metabolic pathway of inorganic arsenicals has yet to be clarified, even though two possible mechanisms have been proposed, i.e., oxidative methylation and glutathione conjugation. AS is primarily excreted in the urine.²¹

AS has been classified as a class I human carcinogen by the International Agency for Research on Cancer (IARC). It is reported that AS has a dual effect on cancer, i.e., it promotes cell proliferation at low concentration, whereas inhibits it at high ones.²² It has also been reported that chronic exposure to AS caused EMT during AS-induced malignant transformation;^{23,24} however, the significance of EMT in AS induced carcinogenesis remains incompletely defined. In our study, we demonstrated that EMT is involved in AS-transformed colon cells.

EMT is considered to be a key early event in tumor invasion and metastasis,²⁵ because EMT converts epithelial cells into

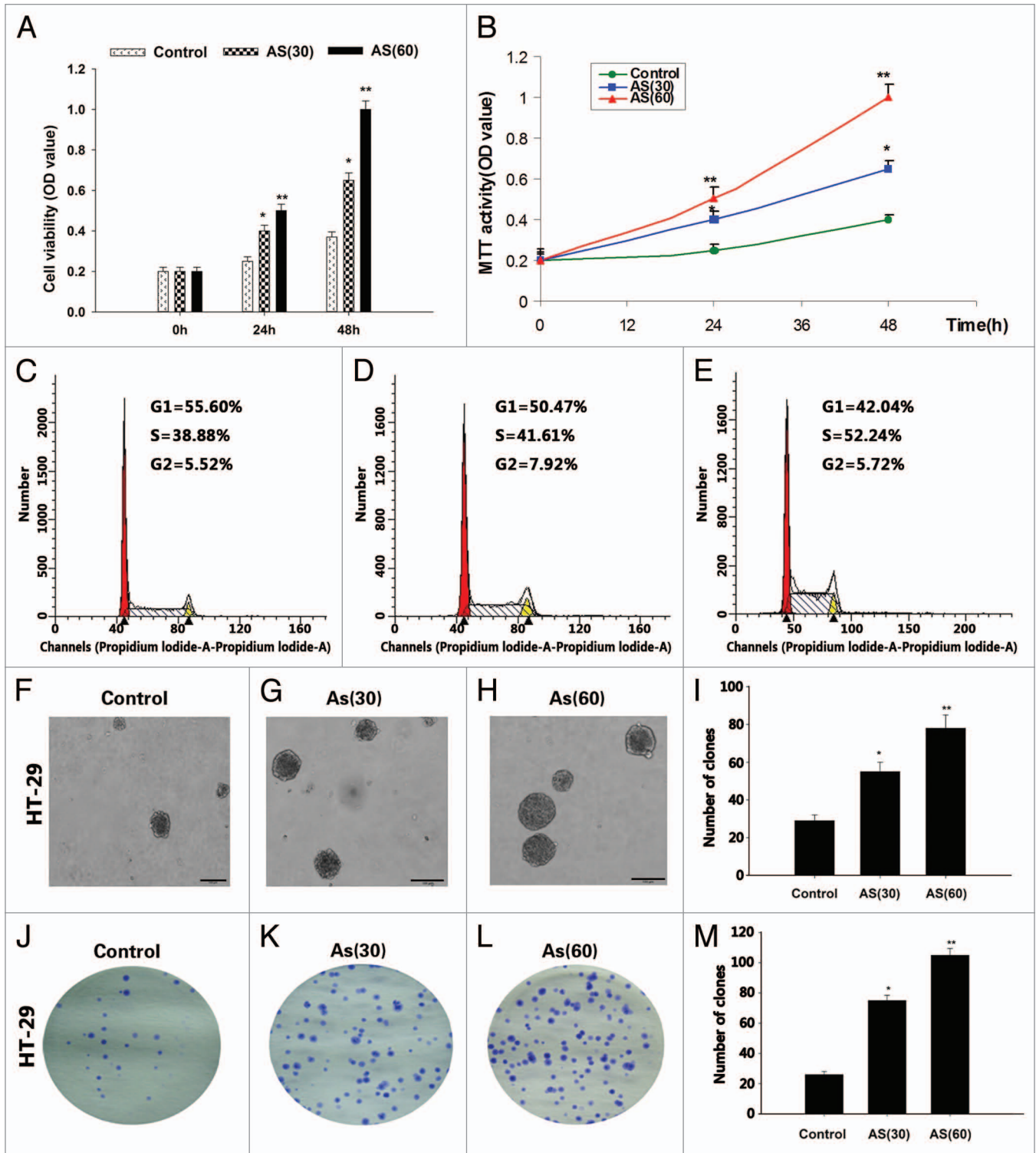


Figure 1. Chronic exposure to AS promotes the proliferation of HT-29 cell lines. (A and B) HT-29 cells were exposed to 0 or 15 nM AS for 0, 30, and 60 passages. In the MTT assay, AS increased the HT-29 cell proliferation, especially in AS (60). * $P < 0.05$; ** $P < 0.01$. (C–E) Similarly, cell cycle analysis suggested that chronic AS treatment accelerated cell re-entering into the S phase. * $P < 0.05$. (F–I) In soft agar culture, chronic AS exposure increased the soft agar colony formation of the HT-29 cells, especially in AS (60) cell. * $P < 0.05$; ** $P < 0.01$. (J–M) Chronic AS exposure increases the plate colony formation rate of the HT-29 cells, especially in AS (60) cell. * $P < 0.05$; ** $P < 0.01$.

mesenchymal-like cells through loss of polarity and disruption of cell–cell connections, which eventually enables cells to become motile and invasive.²⁶ Consistently, studies have shown that the protrusion of podosomes is often found in EMT cancer cells and

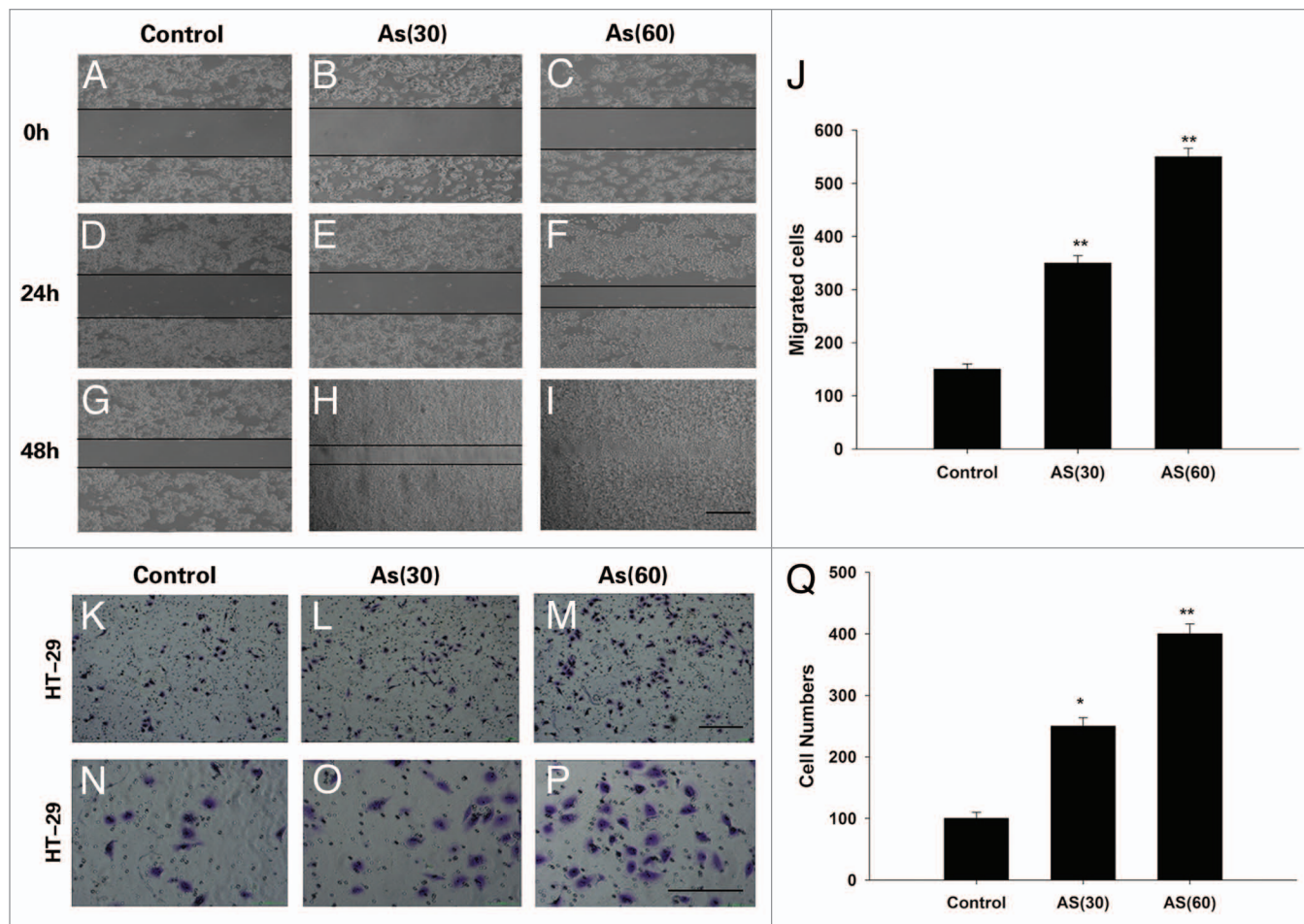


Figure 2. Chronic exposure to AS enhances the migration and invasion of HT-29 cell lines. (A–J) Wound healing rate of HT-29 cell lines at 0, 24, and 48 h after the scratch. AS treated cells, especially the AS (60), migrated much faster than control cells, Note that the wound in AS (60) was nearly closed at 48 h after the scratch (I); bars = 100 μ m. (J) is the quantification of (A–I). (K–Q) Representative crystal violet staining images of cells which attached to the bottom of the transwell filter at 24 h after treatment. (K–M) are the lower power images and (N–P) are the higher power images of (K–M). (Q) The intensity of violet staining was measured as absorbance at 560 nm; bars = 100 μ m in all panels. All experiments were performed 3 times independently, * $P < 0.05$; ** $P < 0.01$.

tumor metastasis.²⁷ Unsurprisingly, in our study, HT-29 cells exposed to AS display a podosphenotype.

Metastasis refers to tumors spread from their initial site to the surrounding normal tissues, and it is responsible for the majority of deaths for cancer patients. It is now known that metastasis is a multistep process and failure of any step may block the entire metastatic process.^{28,29} Although there have been some reports suggested that EMT can promote tumor metastasis both in vitro and in vivo,^{30,31} little is known what low-dose AS would affect colon cancer cells.

In our current study, we focused on how AS promotes cell proliferation and invasion and how AS shift the phenotypes of HT-29 cells from epithelial to mesenchymal. In HT-29 cell lines, proliferation was found to be enhanced in AS-treated cells, as evidenced by increased MTT and the number and size of the colonies. In addition to proliferation, AS also contributes to invasiveness and tumorigenicity, likely through EMT. These data not only provided a strong support for an essential function AS in intestinal tumor cell proliferation and invasion, it also pointed

that EMT is likely a key underlying mechanism. Our findings have great implications in cancer prevention and clinical cancer therapy.

Materials and Methods

Cell culture and reagents

The HT-29 cell line was obtained from the Shanghai Institute of Cell Biology, Chinese Academy of Sciences. Cells were maintained in 5% CO₂ at 37 °C in Dulbecco's modified Eagle's medium (DMEM), supplemented with 10% fetal bovine serum (FBS, Life Technologies/Gibco), 100 U/mL penicillin, and 100 μ g/mL streptomycin (Life Technologies/Gibco). For chronic exposure, 1×10^5 cells were seeded into 6-cm dishes for 12 h and maintained in 0 or 15 nM AS (As₂O₃, Sigma, purity: 99.0%) for 48–72 h per passage. This process was continued for about 15 wk (30 passages) and 30 wk (60 passages). All of the chemicals employed in the present study were of analytical grade.

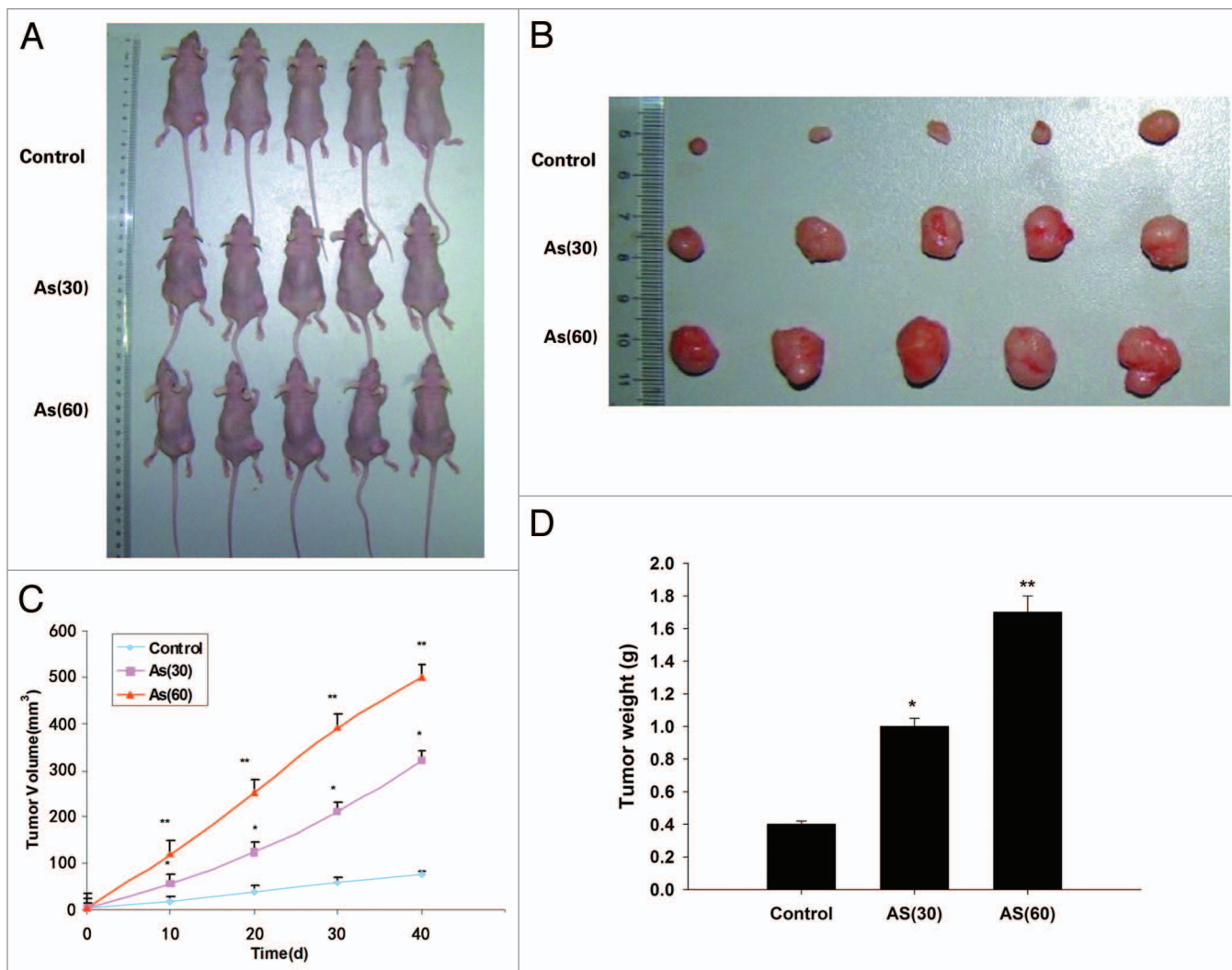


Figure 3. Chronic exposure to AS promotes tumor growth in NOD/SCID mice. **(A and B)** HT-29 cells were exposed to 0 or 15 nM AS for 0, 30, or 60 passages. Representative images of animals **(A)** with subcutaneous implanted tumor, and **(B)** isolated tumors taken on day 40. **(C)** The subcutaneous tumor growth curves. **(D)** Quantification of the tumor weight. * $P < 0.05$; ** $P < 0.01$.

Adhesion assay

AS-treated cells were seeded in 96-well plates (1000 cells/well) for 24 h, followed by washing with sterilized 1× phosphate-buffered saline (PBS) twice and fixing with 70% ethanol for 15 min at room temperature. The adherent cells were evaluated by WST-8 hydrolysis using Cell Counting Kit-8 (CCK-8, Dojindo Molecular Technologies, Inc.), according to manufacturer's instructions.

Western blotting

Western blotting was performed according to the standard procedure. Briefly, the proteins lysates were boiled in the sample-loading buffer, resolved by 6–15% sodium dodecyl sulfate-PAGE (SDS-PAGE) and then transferred to polyvinylidene fluoride membranes (PVDF, Millipore); the immune complexes were detected using an enhanced chemiluminescence kit (Cell Signaling Technology). Primary antibodies used in this study were: E-cadherin, Vimentin, ZEB1, and MMP-9 (Cell Signaling

Technology); β -catenin and MMP-3 (Abcam); β -actin was used as loading control.

Methyl thiazolyl tetrazolium (MTT) assay

AS treated cells were seeded and cultured on 96-well plates at an initial density of 1×10^4 /well. Cell viability was measured by methyl thiazolyl tetrazolium (MTT) assay on hours 0, 24, and 48. All experiments were performed in triplicate. Briefly, 0.02 mL of MTT solution (5 mg/mL in PBS) was added to each well, and incubated for 4 h at 37 °C. Thereafter, the medium was replaced by 0.15 mL of dimethyl sulfoxide for 10 min incubation. The optical density at 570 nm was measured by Microplate spectrophotometer (Thermo Scientific).

Cell cycle analysis

The AS-treated cells were harvested in PBS and fixed in cold ethanol (70%) for overnight. After washed with PBS, cells were permeabilized with 100 μ L RNAase in PBS for 30 min at 37 °C in the absence of light, and then cells were stained with 500 μ L

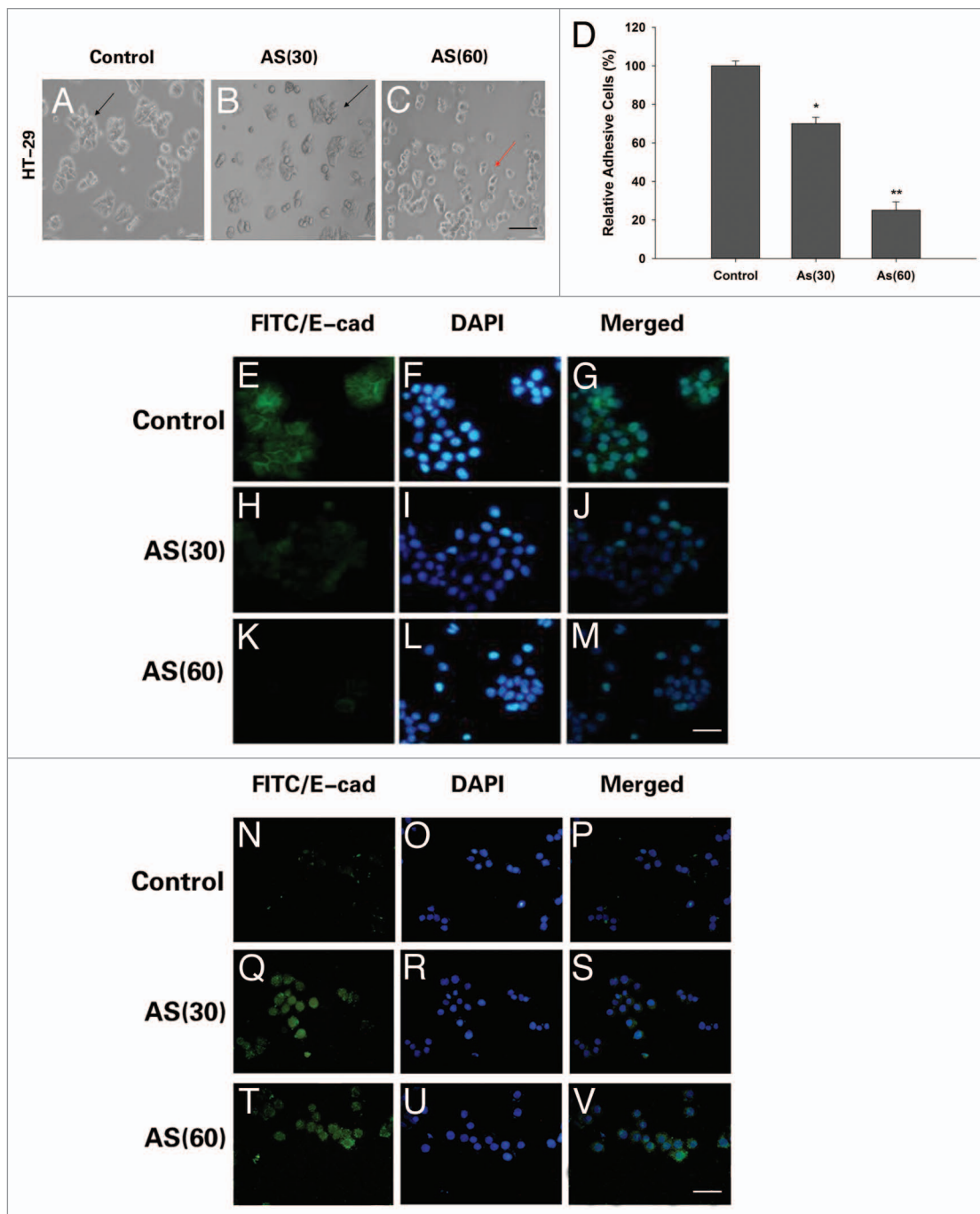


Figure 4. Morphological changes and immunostaining evidences suggested that EMT is involved in the process. (A–C) HT-29 cells were exposed to 0 or 15 nM of arsenic for 0, 30, or 60 passages and typical images with or without AS treatment are shown. Note the morphological shift of HT-29 cells from epithelial-like to mesenchymal-like morphology; Arrows in (A–C) point to the cells with typical morphology. Bars = 100 μ m. (D) Relative adhesion ability of HT-29 cells exposed to AS for 0, 30, or 60 passages; * $P < 0.05$; ** $P < 0.01$. Immunofluorescence staining of E-cadherin (E–M) and vimentin (N–V) in HT-29 cells for the indicated times. (E, H, and K) are green channel that represent E-cadherin staining, and (N, Q, and T) are green channel that represent vimentin staining. (F, I, and L) are blue channel of (E, H, and K), and (O, R, and U) are blue channel of (N, Q, and T), that represents nuclear DNA staining by DAPI, respectively. (G, J, M, P, S, and V) represent merged images; bars = 100 μ m.

of propidium iodide (Sigma) for 30 min. The cell-cycle phases were analyzed by flow cytometry system (Beckman Coulter) at an excitation wavelength of 488 nm and an emission wavelength of 525 nm.

Soft agar assay for colony formation

Five hundred AS-treated cells were re-suspended in 1 mL of complete medium containing 0.7% agar and were then plated on top of a bottom layer that contains 1.2% agar (Sigma) with

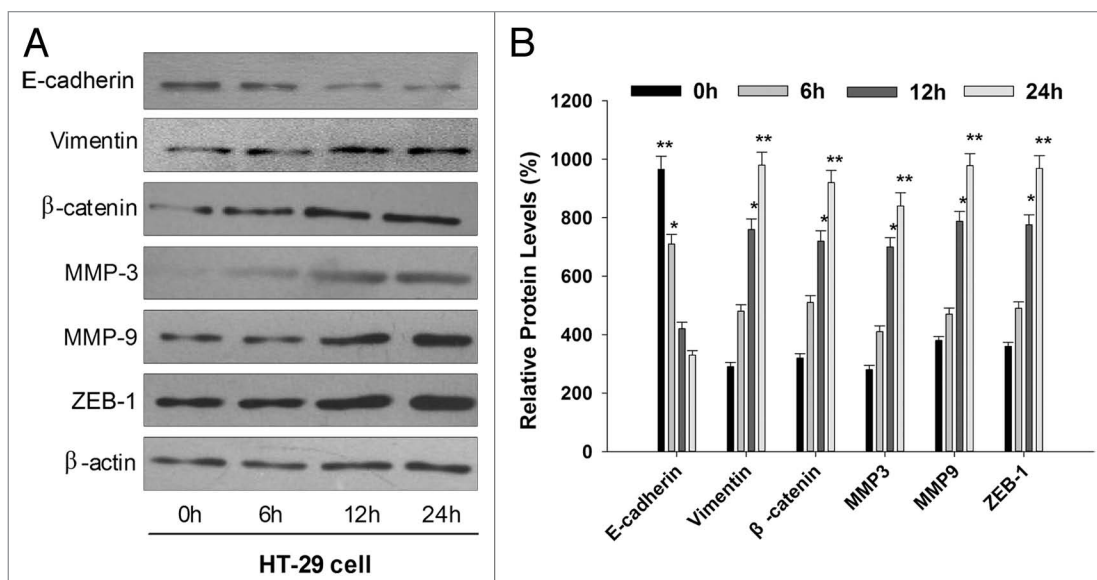


Figure 5. Acute exposure to AS also induces the EMT-like phenotypical shift. (A) HT-29 cells were exposed to 0 or 15 nM arsenic for 0, 6, 12, and 24 h. Western blot was performed to determine the protein expression levels of E-cadherin, vimentin, MMP-3, MMP-9, β-catenin, and ZEB-1. Note that epithelial marker E-cadherin was inhibited by AS, whereas mesenchymal markers (vimentin, MMP-3, and MMP-9) were upregulated. (B) Quantitation of EMT-related proteins in (A), * $P < 0.05$; ** $P < 0.01$.

complete medium. Plates were culture under normal conditions for 2 wk, and then cells colony were counted and photographed under a microscope (Nikon).

Wound-healing assay

AS-treated cells were seeded in six-well plate. Once the full confluence was achieved, a “wound” was made in the middle of a culture plate with a sterile 10 μ L pipette tip and the concentration of the serum in culture medium was then changed from 10% to 2%. The wound-healing process was observed at 0, 24, and 48 h after the scratch under an inverted microscope. The wound healing rate was quantified as the distance of wound recovered over that of the original wound.

Transwell migration and invasion assays

Transwell chambers (polycarbonate filters of 8 μ m porosity, BD Biosciences) were used in this study. A total of 2×10^5 AS treated cells were re-suspended in serum-free medium and plated in the upper chamber or the upper chamber consisting of 8- μ m membrane filter inserts coated with Matrigel (BD Biosciences). After 6–8 h incubation, the cells in the filter side of the upper chamber were cleared with a cotton swab. Cells migrated through the coated membrane were fixed with 4% paraformaldehyde in PBS, followed by 30 min staining of 0.1% crystal violet and then subjected to imaging under 10 \times objective. For further quantification, we cut the filter from the chamber gently, and then the filters were treated with 50% acetic acid was added to each well to dissolve in 0.1% crystal violet and count the migrated cells. The optical density (OD) value was measured using Spectra MAX M5 microplate spectrophotometer (Molecular Devices) at 550 nm and the statistical results of cell numbers per each image field were obtained from three independent experiments averaged from five image fields.

Immunofluorescent and confocal imaging

Immunostaining was performed as described previous report.⁹ Briefly, AS-treated HT-29 cells were grown on glass coverslip until 60–80% confluence, and then fixed and permeabilized with 0.5% Triton-X-100. Rabbit E-cadherin and vimentin antibody were added and incubated at 4 $^{\circ}$ C overnight. After washing, cells were incubated with FITC-conjugated goat-anti-rabbit secondary antibody (1:5000; CWBIO) for 1 h. Then 4',6-diamidino-2-phenylindole (DAPI, Sigma) was added for 10 min to stain the nuclei of HT-29 cells, and the cells were observed under a fluorescence microscope (Olympus, Shinjuku-ku). The images were analyzed with an Image-Pro Plus 6.0 (Olympus).

Xenograft model

To evaluate whether low-dose AS promotes tumor growth in vivo, AS treated or control HT-29 cells (2×10^6) were subcutaneously inoculated into 6-wk-old male athymic mice (5 mice per group) on the flank regions of legs. Tumor nodules were monitored every 3 d, the length and width of the tumors were measured. Tumor volumes were then calculated according to the formula: Volume = width \times length \times (width + length) / 2. On day 40, the mice were euthanized and tumors were harvested. The tumor tissues were weighed and fixed with 4% paraformaldehyde for further histological studies. All animal experiments were approved by the Institute Research Ethics Committee of Anhui Medical University.

Statistical analysis

All values were presented as the mean \pm SEM or median. The χ^2 test or rank test were used for categorical variables, and ANOVA or Student *t* test were used for continuous variables. *indicates $P < 0.05$, **indicates $P < 0.01$. Data were analyzed using the SPSS16.0 software package.

Disclosure of Potential Conflicts of Interest

The authors declare no competing financial interests.

Acknowledgments

This work was supported by the Project of the National Natural Sciences Foundation of China (81272258).

References

1. Cantor KP, Lubin JH. Arsenic, internal cancers, and issues in inference from studies of low-level exposures in human populations. *Toxicol Appl Pharmacol* 2007; 222:252-7; PMID:17382983; <http://dx.doi.org/10.1016/j.taap.2007.01.026>
2. Celik I, Gallicchio L, Boyd K, Lam TK, Matanoski G, Tao X, Shiels M, Hammond E, Chen L, Robinson KA, et al. Arsenic in drinking water and lung cancer: a systematic review. *Environ Res* 2008; 108:48-55; PMID:18511031; <http://dx.doi.org/10.1016/j.envres.2008.04.001>
3. Benbrahim-Tallaa L, Waalkes MP. Inorganic arsenic and human prostate cancer. *Environ Health Perspect* 2008; 116:158-64; PMID:18288312; <http://dx.doi.org/10.1289/ehp.10423>
4. Liu J, Waalkes MP. Liver is a target of arsenic carcinogenesis. *Toxicol Sci* 2008; 105:24-32; PMID:18566022; <http://dx.doi.org/10.1093/toxsci/kfn120>
5. Tapio S, Grosche B. Arsenic in the aetiology of cancer. *Mutat Res* 2006; 612:215-46; PMID:16574468; <http://dx.doi.org/10.1016/j.mrrev.2006.02.001>
6. Tokar EJ, Diwan BA, Waalkes MP. Renal, hepatic, pulmonary and adrenal tumors induced by prenatal inorganic arsenic followed by dimethylarsinic acid in adulthood in CD1 mice. *Toxicol Lett* 2012; 209:179-85; PMID:22230260; <http://dx.doi.org/10.1016/j.toxlet.2011.12.016>
7. Polyak K, Weinberg RA. Transitions between epithelial and mesenchymal states: acquisition of malignant and stem cell traits. *Nat Rev Cancer* 2009; 9:265-73; PMID:19262571; <http://dx.doi.org/10.1038/nrc2620>
8. Xu J, Lamouille S, Derynck R. TGF-beta-induced epithelial to mesenchymal transition. *Cell Res* 2009; 19:156-72; PMID:19153598; <http://dx.doi.org/10.1038/cr.2009.5>
9. Xu Y, Li Y, Pang Y, Ling M, Shen L, Yang X, Zhang J, Zhou J, Wang X, Liu Q. EMT and stem cell-like properties associated with HIF-2 α are involved in arsenite-induced transformation of human bronchial epithelial cells. *PLoS One* 2012; 7:e37765; PMID:22662215; <http://dx.doi.org/10.1371/journal.pone.0037765>
10. Nakamura M, Tokura Y. Epithelial-mesenchymal transition in the skin. *J Dermatol Sci* 2011; 61:7-13; PMID:21167690; <http://dx.doi.org/10.1016/j.jdermsci.2010.11.015>
11. Li Y, Ling M, Xu Y, Wang S, Li Z, Zhou J, Wang X, Liu Q. The repressive effect of NF-kappaB on p53 by mot-2 is involved in human keratinocyte transformation induced by low levels of arsenite. *Toxicol Sci* 2010; 116:174-82; PMID:20375080; <http://dx.doi.org/10.1093/toxsci/kfq109>
12. Lencinas A, Broka DM, Konieczka JH, Klewer SE, Antin PB, Camenisch TD, Runyan RB. Arsenic exposure perturbs epithelial-mesenchymal cell transition and gene expression in a collagen gel assay. *Toxicol Sci* 2010; 116:273-85; PMID:20308225; <http://dx.doi.org/10.1093/toxsci/kfq086>
13. Yang L. Incidence and mortality of gastric cancer in China. *World J Gastroenterol* 2006; 12:17-20; PMID:16440411
14. Saika K, Sobue T. [Cancer statistics in the world]. *Gan To Kagaku Ryoho* 2013; 40:2475-80; PMID:24335357
15. Hutchings SJ, Rushton L. Occupational cancer burden in Great Britain. *Br J Cancer* 2012; 107:S92-103; PMID:22710685; <http://dx.doi.org/10.1038/bjc.2012.123>
16. Fernández-Navarro P, García-Pérez J, Ramis R, Boldo E, López-Abente G. Proximity to mining industry and cancer mortality. *Sci Total Environ* 2012; 435-436:66-73; PMID:22846765; <http://dx.doi.org/10.1016/j.scitotenv.2012.07.019>
17. He C, Chen M, Liu J, Yuan Y. Host genetic factors respond to pathogenic step-specific virulence factors of *Helicobacter pylori* in gastric carcinogenesis. *Mutat Res Mutat Res* 2014; 759:14-26; PMID:24076409; <http://dx.doi.org/10.1016/j.mrrev.2013.09.002>
18. Akhavan-Niaki H, Samadani AA. Molecular Insight in Gastric Cancer Induction: An Overview of Cancer Stemness Genes. *Cell Biochem Biophys* 2014; 68:463-73 PMID:24078401
19. Barrett JR. A potential window onto early pancreatic cancer development: evidence of cancer stem cell growth after exposure to cadmium chloride in vitro. *Environ Health Perspect* 2012; 120:A363; PMID:23487843; <http://dx.doi.org/10.1289/ehp.120-a363a>
20. Huang HH, Huang JY, Lung CC, Wu CL, Ho CC, Sun YH, Ko PC, Su SY, Chen SC, Liaw YP. Cell-type specificity of lung cancer associated with low-dose soil heavy metal contamination in Taiwan: an ecological study. *BMC Public Health* 2013; 13:330; PMID:23575356; <http://dx.doi.org/10.1186/1471-2458-13-330>
21. Watanabe T, Hirano S. Metabolism of arsenic and its toxicological relevance. *Arch Toxicol* 2013; 87:969-79; PMID:22811022; <http://dx.doi.org/10.1007/s00204-012-0904-5>
22. Snow ET, Sykora P, Durham TR, Klein CB. Arsenic, mode of action at biologically plausible low doses: what are the implications for low dose cancer risk? *Toxicol Appl Pharmacol* 2005; 207(Suppl):557-64; PMID:15996700; <http://dx.doi.org/10.1016/j.taap.2005.01.048>
23. Wang Z, Zhao Y, Smith E, Goodall GJ, Drew PA, Brabletz T, Yang C. Reversal and prevention of arsenite-induced human bronchial epithelial cell malignant transformation by microRNA-200b. *Toxicol Sci* 2011; 121:110-22; PMID:21292642; <http://dx.doi.org/10.1093/toxsci/kfr029>
24. Jiang R, Li Y, Xu Y, Zhou Y, Pang Y, Shen L, Zhao Y, Zhang J, Zhou J, Wang X, et al. EMT and CSC-like properties mediated by the IKK β /I κ B α /RelA signal pathway via the transcriptional regulator, Snail, are involved in the arsenite-induced neoplastic transformation of human keratinocytes. *Arch Toxicol* 2013; 87:991-1000; PMID:23069812; <http://dx.doi.org/10.1007/s00204-012-0933-0>
25. Thiery JP, Aclouche H, Huang RY, Nieto MA. Epithelial-mesenchymal transitions in development and disease. *Cell* 2009; 139:871-90; PMID:19945376; <http://dx.doi.org/10.1016/j.cell.2009.11.007>
26. Lee JM, Dedhar S, Kalluri R, Thompson EW. The epithelial-mesenchymal transition: new insights in signaling, development, and disease. *J Cell Biol* 2006; 172:973-81; PMID:16567498; <http://dx.doi.org/10.1083/jcb.200601018>
27. Eckert MA, Lwin TM, Chang AT, Kim J, Danis E, Ohno-Machado L, Yang J. Twist1-induced invadopodia formation promotes tumor metastasis. *Cancer Cell* 2011; 19:372-86; PMID:21397860; <http://dx.doi.org/10.1016/j.ccr.2011.01.036>
28. Fidler IJ. The pathogenesis of cancer metastasis: the 'seed and soil' hypothesis revisited. *Nat Rev Cancer* 2003; 3:453-8; PMID:12778135; <http://dx.doi.org/10.1038/nrcl098>
29. Weiss L. Metastasis of cancer: a conceptual history from antiquity to the 1990s. *Cancer Metastasis Rev* 2000; 19:1-XI, 193-383; PMID:11394186
30. Cooke VG, LeBleu VS, Keskin D, Khan Z, O'Connell JT, Teng Y, Duncan MB, Xie L, Maeda G, Vong S, et al. Pericyte depletion results in hypoxia-associated epithelial-to-mesenchymal transition and metastasis mediated by met signaling pathway. *Cancer Cell* 2012; 21:66-81; PMID:22264789; <http://dx.doi.org/10.1016/j.ccr.2011.11.024>
31. Wang L, Wu Y, Lin L, Liu P, Huang H, Liao W, Zheng D, Zuo Q, Sun L, Huang N, et al. Metastasis-associated in colon cancer-1 upregulation predicts a poor prognosis of gastric cancer, and promotes tumor cell proliferation and invasion. *Int J Cancer* 2013; 133:1419-30; PMID:23457029; <http://dx.doi.org/10.1002/ijc.28140>